Journal of Molecular Graphics and Modelling 53 (2014) 212–220

Contents lists available at ScienceDirect

Journal of Molecular Graphics and Modelling

journal homepage: www.elsevier.com/locate/JMGM

Mechanism and regioselectivity of the reversible Diels–Alder cycloaddition of 2-methyl-1,3 butadiene with $C_{48}B_6N_6$ heterofullerene: A DFT approach

Ehsan Zahedi*

Chemistry Department, Shahrood Branch, Islamic Azad University, Shahrood, Iran

ARTICLE INFO

Article history:
Accepted 21 August 2014
Available online 29 August 2014

Keywords:
Diels–Alder cycloaddition
DFT
$C_{48}B_6N_6$
Regioselectivity
Fukui function

ABSTRACT

A theoretical study of the mechanism and regioslectivity of Diels–Alder [4+2] cycloaddition reactions between 2-methyl-1,3 butadiene and hetero bonds of the most stable isomer of $C_{48}B_6N_6$ heterofullerene have been studied at the B3LYP/6-31G* level. Three heterobond pathways B—C, B—N and N—C including two regioisomers for each one are considered by different approaches. All studied reactions have normal electron demand nature and corresponding regioisomers are produced via asynchronous processes. Predicted regioselectivities using electronic and energetic results are in complete agreement with each other and show that B—C heterobond pathway is more active than others and regioisomer **16** is the major. The local reactivity difference values (R_k) show that all reaction sites at $C_{48}B_6N_6$ present ambiphilic activation while reaction sites at 2-methyl-1,3 butadiene show nucleophilic activation. Therefore, it is predictable that $C_{48}B_6N_6$ should present electrophilic nature. Plotting of ΔR_k and Δs values of six studied channels toward corresponding activation Gibbs free energies showed that the regioisomeric channel with lower ΔR_k and Δs values is faster and *vice versa*.

1. Introduction

Buckminsterfullerene is a curved polyhedral clusters of carbon comprising fused pentagonal and hexagonal rings. C_{60} is the most prominent representative of the fullerene family. Preparation of bulk quantities of C_{60} is invented by Krätschmer and co-workers [1] via arc-discharge method. It has full icosahedral symmetry (I_h) included 12 pentagons separated by 20 fused hexagons so that, based on isolated pentagon rule (IPR), none of the pentagons are in contact with each other [2]. Electronic, magnetic, and chemical properties of C_{60} can be manipulated via incorporation of heteroatom into the fullerene skeleton. On-ball doping of C_{60} by BN units makes the multi component system isoelectronic to the parent fullerene with the general formula of $C_{60-2n}B_nN_n$ (known as heterofullerene) [2,3]. Despite the extended aromatic stability of heterofullerenes, this molecule is quite reactive [4]. The torsionally strained π-electron system, due to the spherical shape of heterofullerenes, gives an electron-withdrawing nature which enables them to react with electron-rich reagents [5]. Heterofullerene and fullerene as electron deficient systems can participate in the various types of reactions such as reduction, nucleophilic addition, hydrogenation, halogenation, radical addition, and cycloaddition [6–8]. Among them, cycloaddition reactions are the most important reactions for functionalization of heterofullerene and fullerene. A number of cycloaddition reactions including [1+2], [2+2], [3+2], [4+2], [6+2], and [8+2] have been reported but the [4+2] Diels–Alder cycloaddition (**42C**) reaction has been the most employed reaction for the preparation of novel organofullerenes [9–12]. In fact **42C** reactions provide the most successful method for the functionalization of fullerene-based cages and preparation of its derivatives. From the viewpoint of history the first **42C** reaction of C_{60} using o-quinodimethane and its analogs as reactive dienes were reported by Belik et al. [13] and Rubin et al. [14]. Recently **42C** reaction of fullerene-based materials has been extensively studied experimentally and theoretically. Yang et al. [15] studied the hetero **42C** reaction of C_{60} with nitrosoalkene to prepare a new type of stable C_{60}-fused dihydrooxazine derivatives. Afterwards, Yang et al. [16] reported an unusual C—C and C—O bond cleavage of ketoxime in their reaction with C_{60}. This property prepare suitable conditions for C_{60} to participate in the two different cycloaddition reactions, simultaneously. C—C bond cleavage of ketoxime produces nitrile oxide intermediate that is an active molecule for 1,3-dipolar cycloaddition (**32C**) while C—O bond cleavage results nitrosoethene intermediate, which is

* Tel.: +98 9122733755; fax: +98 23 32344634.
E-mail addresses: e_zahedi1357@yahoo.com, e_zahedi@iau-shahrood.ac.ir

http://dx.doi.org/10.1016/j.jmgm.2014.08.003
1093-3263/

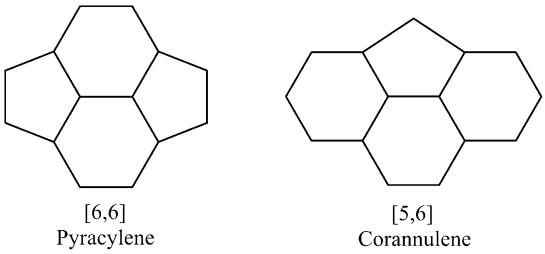

Fig. 1. Different bond types in the pristine fullerene (C_{60}).

capable for hetero **42C** reaction with C_{60}. Takahashi et al. [17] reported first example of the diastereoselective **42C** reaction of C_{60} with dendron. They isolated and confirmed fullerodendrons (−)-4L and (+)-4D from the mixture of diastereomers by ^{1}H and ^{13}C NMR spectroscopy, FT-IR, and MALDI-TOF mass spectroscopic analysis. Effect of the encapsulated metals on the reactivity of fullerene cages and its mechanism is the other interested field in the chemical functionalization of fullerenes via **42C** reactions [18–20].

Since the **42C** reactions are highly regioselective, the regiocontrol study of exohedral functionalization of fullerene-based cages is important. In view of the fact that fullerenes are electron deficient in nature, double bonds act as 2π electron electrophile and consequently fullerene-based cages are ideal dienophile for undergoing **42C** reactions. The pristine fullerene (C_{60}) has two types of bonds between carbon atoms, namely **[6,6]** or pyracylene and **[5,6]** or corannulene bonds (Fig. 1). **[6,6]** bond is shared bond between two hexagonal rings whereas **[5,6]** bond is shared bond between a hexagonal and a pentagonal rings. Previous studies show that the **[6,6]** bonds are good dienophiles with respect to **[5,6]**. This is due to the bonding and antibonding nature of π orbitals of **[6,6]** and **[5,6]** bonds in the high occupied molecular orbital (HOMO) of pristine fullerene (C_{60}), respectively. This property causes the larger π-electron density and shorter **[6,6]** bond in comparison with **[5,6]** bond [11,21–26]. In the heterofullerenes, regioselectivity subject is different because contrary to C_n-fullerenes that have only C—C bonds heterofullerenes have hetero bonds (X—Y). Therefore, regioselectivity prediction of **42C** reactions of unsymmetrical dienes with hetero bonds of heterofullerenes (as unsymmetrical dienophile) is other kind of looking to the regioselectivity subject in the fullerene chemistry and has never been done before. Hence, this project provides a detailed description of regioselectivity of **42C** reaction between 2-methyl-1,3 butadiene and hetero bonds of the most stable isomer of $C_{48}B_6N_6$ heterofullerene [4,27] by means of several theoretical approaches.

2. Computational method and theoretical background

The initial geometry of C_{60} was used to construct $C_{48}B_6N_6$ by replacing 6 carbon atoms by nitrogen atoms and another 6 carbon atoms by boron atoms (Fig. 2). All geometry optimizations and electronic analysis were carried out using the B3LYP exchange-correlation functionals [28,29], together with the standard 6-31G* basis set [30]. Optimizations of both minimum and transition states (TSs) were done using the Berny analytical gradient algorithm [31]. The stabilities of restricted DFT (density functional theory) wave functions toward unrestricted alternatives for optimized structures were tested using STABLE keyword [32] and instability was not found. To confirm the nature of the stationary species and compute the thermodynamic parameters, frequency calculations were carried out at 298.15 K and 1.0 atm. For minimum state structures, only real frequency values, and for the TSs only a single imaginary frequency value corresponding to the vibration of the two new formed

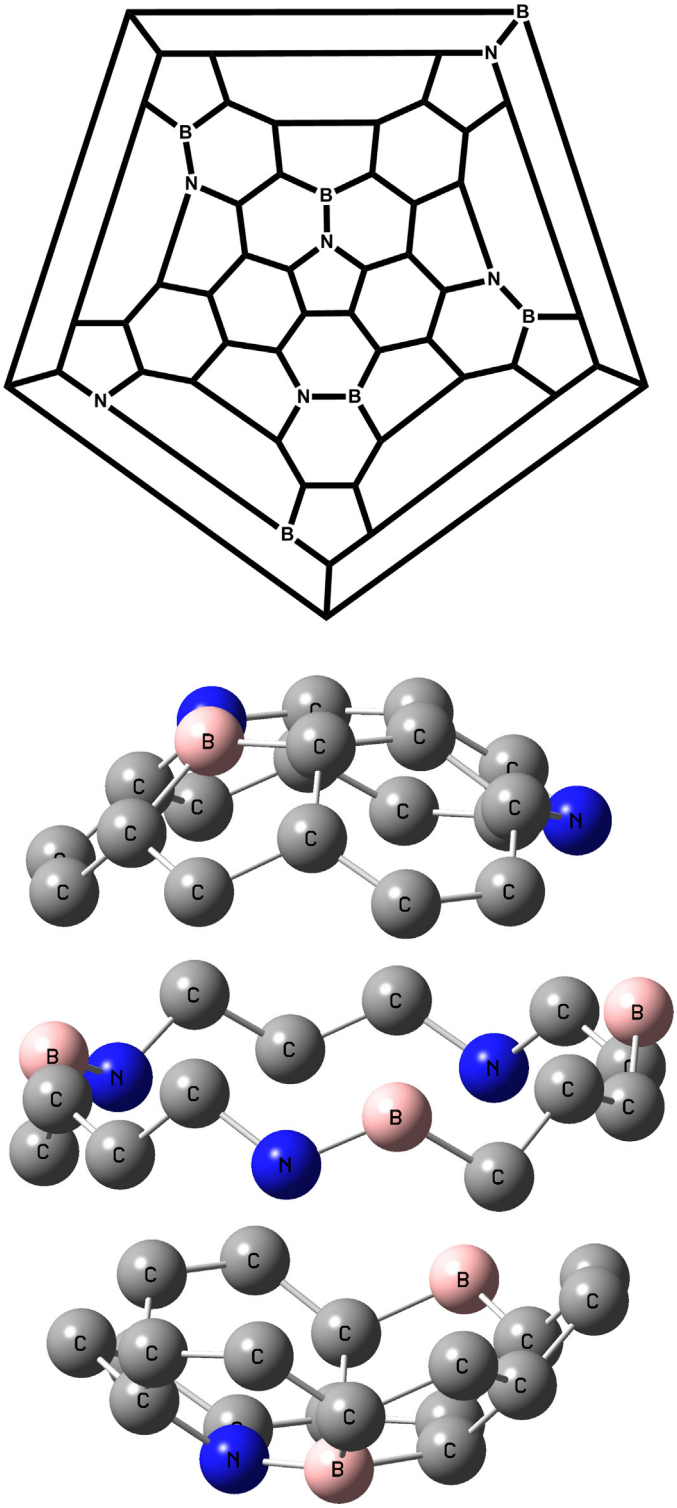

Fig. 2. Schlegel diagram of $C_{48}B_6N_6$ and its broken 3D structure into three units.

bonds were accepted. All calculations were carried out with the Gaussian 09 suite of program [33].

Reactivity indices based on the conceptual DFT framework such as global electrophilicity (ω), local electrophilicity (ω_k), global nucleophilicity (N), local nucleophilicity (N_k) and R_k index are powerful tools in order to understand the molecular reactivity at the ground states.

Parr et al. [34] have defined the global electrophilicity ($\omega = \mu^2/2\eta$) as stabilization energy of a molecule when it gains an

additional charge from the environment, where, μ^2 is the electrophile ability to capture an amount of extra charge and η is the resistance of a molecule to exchange charge with the environment [35]. Electronic chemical potential, μ, and absolute hardness, η, are the first and second derivatives of the total energy with respect to the electron number N at a constant external potential $v(r)$, respectively, in such a manner that based on the Koopmans' can be rewritten as:

$$\mu = \left(\frac{\partial E}{\partial N}\right)_v \approx \frac{1}{2}(E_{\mathrm{HOMO}} + E_{\mathrm{LUMO}})$$

$$\eta = \left(\frac{\partial^2 E}{\partial N^2}\right)_v = \left(\frac{\partial \mu}{\partial N}\right)_v \approx (E_{\mathrm{LUMO}} - E_{\mathrm{HOMO}})$$

where E_{HOMO} and E_{LUMO} are the frontier molecular orbital energies [35,36]. Organic molecules may be classified as strong electrophiles with $\omega > 1.5$ eV, moderate electrophiles with $1.5 < \omega < 0.8$ eV, and marginal electrophiles, $\omega < 0.8$ eV [37].

Recently, Chattaraj et al. [35] and Domingo et al. [38,39] introduced an empirical (relative) nucleophilic index, N, for closed shell organic molecules based on the E_{HOMO} of nucleophile referred to the E_{HOMO} of tetracyanoethylene (TCE) as follows:

$$N = E_{\mathrm{HOMO(Nu)}}\,(\mathrm{eV}) - E_{\mathrm{HOMO(TCE)}}\,(\mathrm{eV})$$

TCE has the lowest E_{HOMO} in a large series of molecules and guarantees positive nucleophilicity value. Organic molecules can be classified as strong nucleophiles with $N > 3.0$ eV, moderate nucleophiles with $3.0 \leq N \leq 2.0$ eV, and marginal nucleophiles, $N < 2.0$ eV [40].

Local electrophilicity (ω_k), and local nucleophilicity (N_k) at the atomic site k can be defined in terms of related condensed Fukui functions, f_k^+ and f_k^- as:

$$\omega_k = \omega \cdot f_k^+$$

and

$$N_k = N \cdot f_k^-$$

Fukui function is an important concept in conceptual DFT and useful local reactivity indicator. Fukui function is the first derivative of the electronic density $\rho(r)$ of a system with respect to the number of electrons at a constant external potential $v(r)$ [41]:

$$f(r) = \left[\frac{\partial \rho(r)}{\partial N}\right]_v$$

Yang and Mortier [42] proposed the condensed form of Fukui functions in terms of the variation of gross charges of an atom, say k, in a molecule with N electrons as:

$$f_k^+ = [q_k(N+1) - q_k(N)] \quad \text{for nucleophilic attack}$$

$$f_k^- = [q_k(N) - q_k(N-1)] \quad \text{for electrophilic attack}$$

In the present study Fukui function values are calculated using Hirshfeld's population because Hirshfeld charges guaranty the positive Fukui function values [43,44].

Very recently, Chattaraj et al. [35] proposed a new local reactivity difference index namely, R_k, which is capable to predict the local electrophilic and/or nucleophilic activation sites in the organic molecule as:

(1) If $(1 < \omega_k/N_k < 2)$ or $(1 < N_k/\omega_k < 2)$ then $R_k \approx (\omega_k + N_k)/2 \Rightarrow$ ambiphilic ($R_k = \pm n.nn$).
(2) Else $R_k \approx (\omega_k - N_k)$ where $R_k > 0 \Rightarrow$ electrophilic ($R_k = +n.nn$) and $R_k < 0 \Rightarrow$ nucleophilic ($R_k = -n.nn$).
(3) If $|R_k| < 0.10$, then $R_k = 0.00$.

In the R_k index, the sign indicates the nature of the center k and the magnitude $n.nn$ provides a measure of the local activation. Electrophilic and ambiphilic active sites can be classified as strong with $|R_k| > 0.7$ eV, moderate with $0.4 < |R_k| > 0.7$ eV and marginal $|R_k| < 0.4$ eV while nucleophilic active sites can be classified as strong with $|R_k| > 1.5$ eV, moderate with $|1.0 < R_k| < 1.5$ eV and marginal $|R_k| < 1.0$ eV.

3. Results and discussion

In the structure of $C_{48}B_6N_6$ there are six B—N heterobonds that all of them are equivalent from viewpoint of neighboring atoms. Each boron or nitrogen atoms are connected to two carbon atoms, then in each one of the $C_{48}B_6N_6$ doped positions there are three heterobonds B—C, B—N, and N—C. Because of similarity between $C_{48}B_6N_6$ doped positions only **42C** reactions of 2-methyl-1,3 butadiene and heterobonds of one doped position, including three heterobond pathways B—C, B—N, and N—C, are investigated. In each of the mentioned heterobond pathways, two regioisomers can be generated, regiosomers **15** and **16** in the heterobond pathway B—C, regiosomers **25** and **26** in the heterobond pathway B—N, regiosomers **35** and **36** in the heterobond pathway N—C (Fig. 3). The PES (Potential Energy Surface), relative Gibbs free energies, and geometric structures of transition states corresponding to all channels are illustrated in Fig. 4. It turns out from the calculated activation Gibbs free energies ($\Delta G^{\ddagger}$) that the most favorable reactive channels correspond to the **42C** reactions of 2-methyl-1,3 butadiene and B—C heterobond via regioisomeric channels **15** and **16**. The values of relative Gibbs free energies with respect to the separate reactants for **TS15** and **TS16** are 23.36 and 20.74 kcal/mol, respectively. These values show that **TS16** is 2.62 kcal/mol more favorable than **TS15**. The activation Gibbs free energies associated with the **42C** reactions of 2-methyl-1,3 butadiene and B—N heterobond are 25.83 (**TS25**) and 29.24 (**TS26**) kcal/mol, while for N—C heterobond are 56.23 (**TS35**) and 52.72 (**TS36**) kcal/mol. On the whole B—C and N—C heterobonds are the most active and inactive heterobonds for **42C** reaction, respectively, and channel **16** is associated to the most favorable regioisomer. Due to the unfavorable activation Gibbs free energies (>25 kcal/mol), it seems that **42C** reactions of 2-methyl-1,3 butadiene and B—N/N—C heterobonds cannot carried out experimentally in laboratories. All considered **42C** reactions are endothermic and regioisomer **16** is more stable than the others. Positive Gibbs free energies of reactions (ΔG) indicate that all cycloadducts are thermally unstable and easily cycloreverse to the component molecules upon heating. Instability of cycloadducts is due to loss of aromaticity of $C_{48}B_6N_6$ [45]. The calculated activation Gibbs free energies and Gibbs free energies of reactions are qualitatively comparable.

Analysis of the geometries of the TSs involved in the studied **42C** reactions indicate that these reactions take place via asynchronous concerted TSs. The lengths of the two sigma bonds formed in the studied TSs are given in Fig. 4. The degree of the synchronicity (Δr) can be measured as the difference between the lengths of the mentioned two sigma bonds. For the heterobond pathway B—N the measured asynchronicities are smaller than other heterobonds. Δr values for **TS25** and **TS26** are 0.418 and 0.445 Å, respectively, whereas for **TS16** and **TS15** are 0.646 and 0.677 Å, and for **TS36** and **TS35** are 0.549 and 0.611 Å, respectively. Therefore the least asynchronicity nature is observed for **TS25**, and in each of the

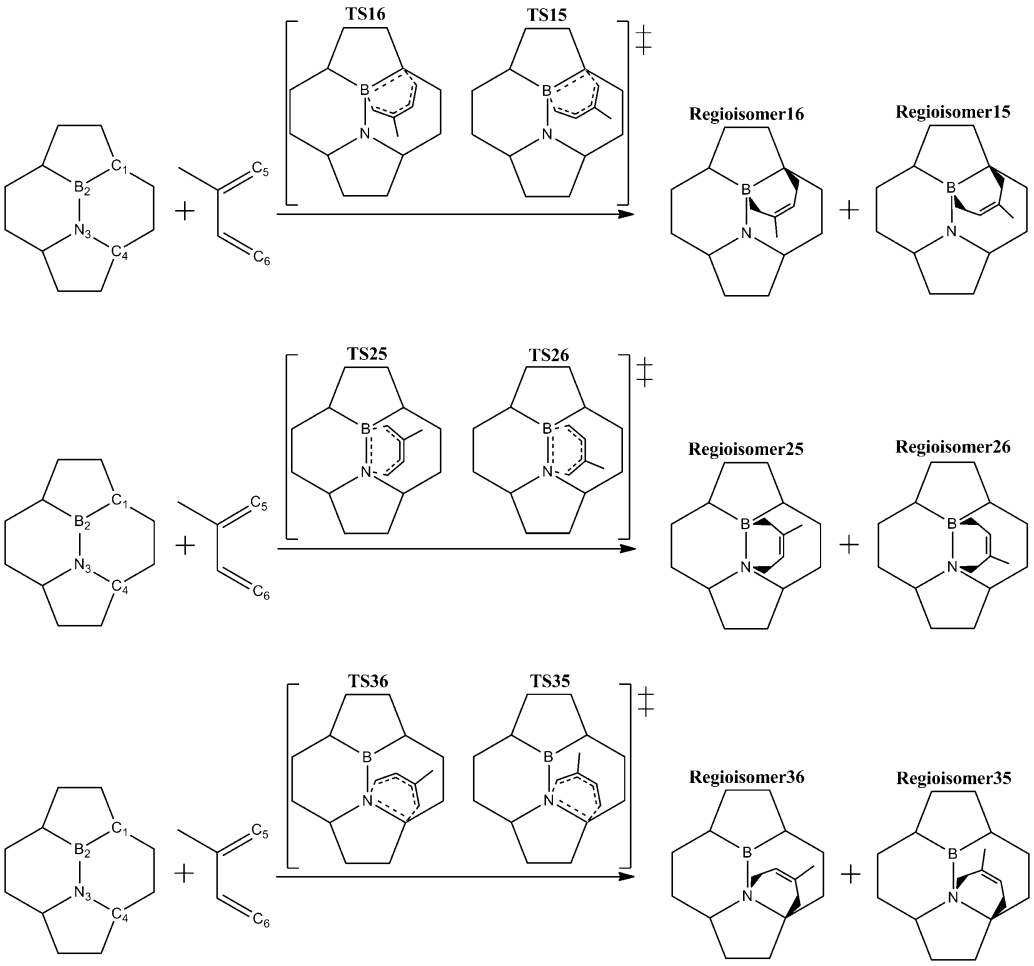

Fig. 3. Heterobond pathways (B—C, B—N and N—C) and regioisomeric channels for **42C** reaction between 2-methyl-1,3 butadiene and $C_{48}B_6N_6$ heterofullerene.

heterobond pathways the favorable TS, from the viewpoint of energy, is more synchronous than the other. Values of the two forming sigma bonds indicates that formation of the B—C bonds in the **TS15**, **TS16**, **TS25**, and **TS26** are more advanced than other, while in the **TS35** and **TS36** formation of the C—C bonds are more advanced than the N—C bonds. The mechanism of the studied reactions and polar nature of TSs are evaluated by analyzing the Hirshfeld charge transfer (CT) at the TSs. In all TSs, the charge is transferred from the donor 2-methyl-1,3 butadiene to the acceptor $C_{48}B_6N_6$ and show that all studied reactions have normal electron demand (NED) character. The CT values at the corresponding TSs are between 0.17 and 0.28ē (Fig. 4) and allow to classify studied **42C** reactions as polar [46]. The CT for **TS36** and **TS35** are 0.28 and 0.25ē, respectively, by contrast the shared atomic charges for **TS25** and **TS26** are 0.19 and 0.18ē, and for **TS16** and **TS15** are 0.18 and 0.17ē, respectively. The order of CT values in the three heterobond pathways are as N—C > B—N > B—C in such a manner that the same order is observed for activation Gibbs free energies and Gibbs free energies of reactions. In order to justify the observed behavior, Coulson MO bond orders of N—C, B—N, and B—C heterobonds of pristine $C_{48}B_6N_6$ have been computed by using the NBO analysis as implemented in Gaussian program (NBO 3.1, Link 607) [47]. Coulson MO bond orders of N—C, B—N, and B—C heterobonds are 1.51, 1.32, and 1.24, respectively. Bond order values show that the B—C bond is good dienophile with respect to the B—N and N—C bonds and regularly its tendency to accept electron is less than the other heterobonds. By contrast bond order of N—C bond is the least therefore its tendency to accept electron in order to redresses π electron deficiency is significant. For these matters B—C heterobond channels are more active than the B—N and N—C bonds.

Taking into account the observations obtained from energetic results and in order to justify the results from electronic point of view, reactivity indices defined in the theoretical background should be considered. Frontier molecular orbital (FMO) energies, electronic chemical potential, chemical hardness, global electrophilicity, and global nucleophilicity indices of reactants are calculated and given in Table 1. The electronic chemical potential of 2-methyl-1,3 butadiene is higher than $C_{48}B_6N_6$ and indicate that the electron flux takes place from the 2-methyl-1,3 butadiene to $C_{48}B_6N_6$. This behavior is in agreement with the observed direction of electron flux in the transition states structures (Fig. 4) and allows to classify studied reactions as NED. Global electrophilicity values of reactants allow to classify the $C_{48}B_6N_6$ as a strong electrophile and 2-methyl-1,3 butadiene as a moderate electrophile. Therefore, $C_{48}B_6N_6$ can act as an electrophile and 2-methyl-1,3 butadiene act as a nucleophile. This consequence is in agreement with electron deficient

Table 1
FMO energies (a.u.), electronic chemical potential (eV), chemical hardness (eV), global electrophilicity (eV) and global nucleophilicity (eV) of reactants.

	HOMO	LUMO	μ	η	ω	N^a
$C_{48}B_6N_6$ Heterofullerene	−0.206	−0.113	−4.34	2.53	3.72	3.51
2-Methyl-1,3 butadiene	−0.227	−0.015	−3.29	5.76	0.94	2.94

[a] E_{HOMO}(TCE) = 0.335 a.u.

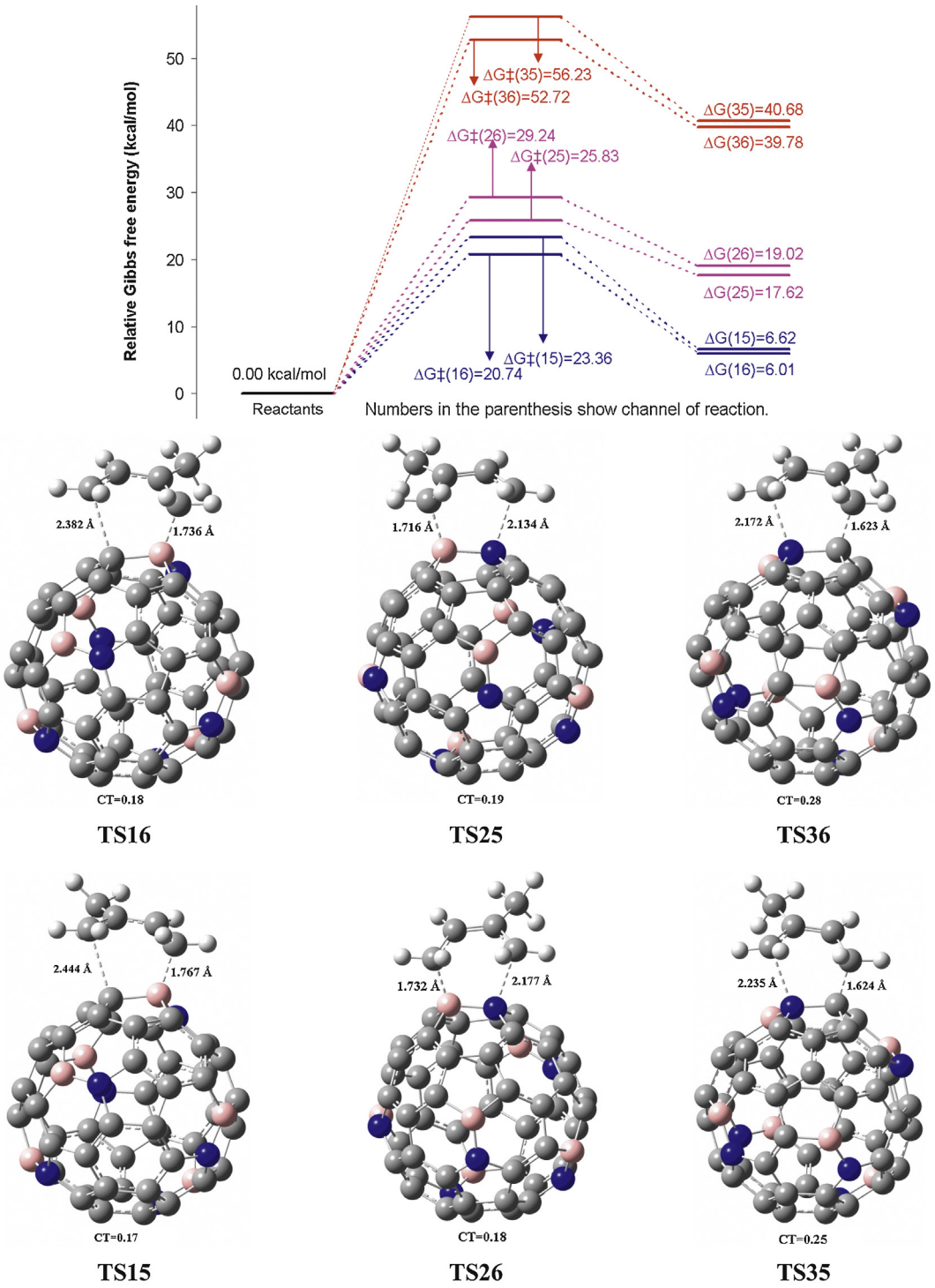

Fig. 4. Energy profile, in kcal/mol, for the studied **42C** reactions and B3LYP/6-31G* optimized geometries of corresponding TSs. Formed sigma bonds are in Å and charge transfer values (CT) are in ē units.

nature of $C_{48}B_6N_6$, orientation of electron flux in the transition states structures and NED character of studied reactions. Analysis of HOMO–LUMO energy gap between reactants for **42C** reactions of 2-methyl-1,3 butadiene and heterobonds of $C_{48}B_6N_6$ is comprising of graphical knowledge about molecular orbitals in the considered heterobonds and diene. It should be noted that HOMO and LUMO orbitals are those which involved directly in the reaction (relevant HOMO and LUMO) and not necessarily the highest occupied molecular orbital or the lowest unoccupied molecular orbital (actual HOMO and LUMO). For each heterobonds of $C_{48}B_6N_6$, two π electrons exist therefore relevant HOMO should be extended on the considered heterobonds without any node but relevant LUMO must have one node between two considered heteroatoms. By contrast in the 2-methyl-1,3 butadiene 4 π electrons exist, consequently relevant HOMO and LUMO must have one and two nodes, respectively. In the studied reactions, the relevant HOMO and actual HOMO of 2-methyl-1,3 butadiene are the same. Possible interactions between relevant orbitals of 2-methyl-1,3 butadiene and heterobonds of

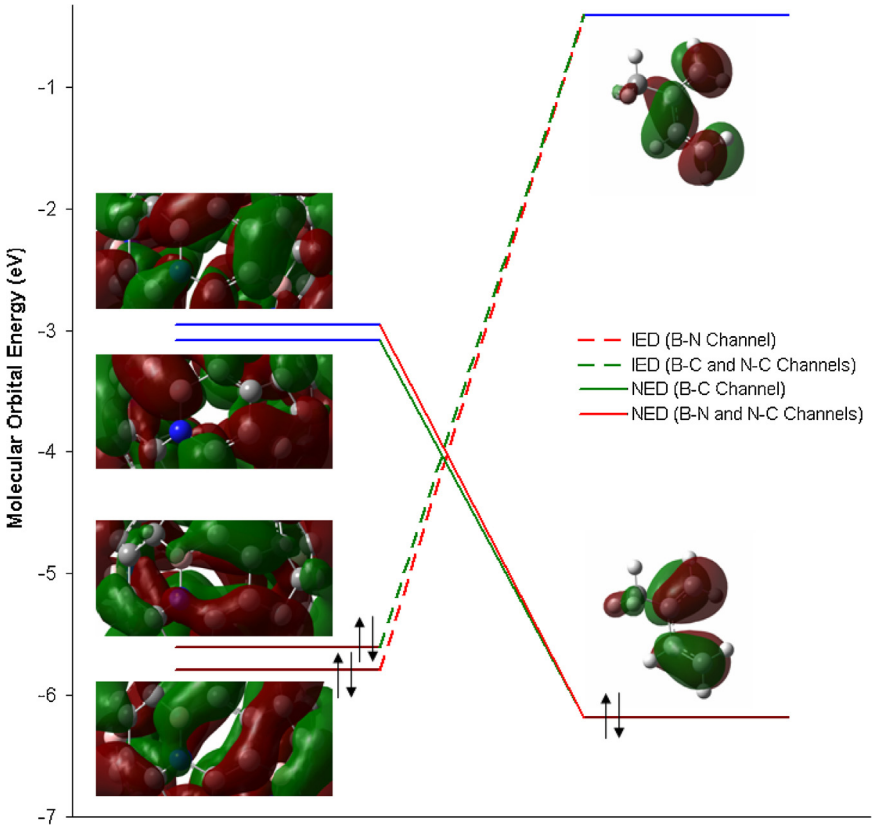

Fig. 5. A schematic representation of two possible HOMO–LUMO interactions of reactants in each of heterobond pathways as proposed by the FMO theory.

$C_{48}B_6N_6$ are sketched in Fig. 5. Visualized relevant HOMO and LUMO orbitals are included in Fig. 5 for better understanding. Possible interactions between relevant molecular orbitals of reactants in the three heterobond pathways show that the favor interaction occurs between relevant HOMO orbital of 2-methyl-1,3 butadiene and relevant LUMO orbital of considered heterobonds of $C_{48}B_6N_6$. This prediction confirms NED nature of considered reactions and orientation of electron flux in the corresponding TSs. In continuation, in order to consider the mechanism of studied reactions carefully, local electrophilicity, local nucleophilicity and local reactivity difference indices for reaction sites should be investigated. The corresponding values are calculated using Yang and Mortier (Y M) Fukui functions which are tabulated in Table 2. Analysis of the local reactivity difference shows that all reaction sites (C_1, B_2, N_3 and C_4) at $C_{48}B_6N_6$ present ambiphilic activation while reaction sites at 2-methyl-1,3 butadiene (C_5, C_6 and carbon atoms connected to them) show nucleophilic activation. In the presence of nucleophilic centers of 2-methyl-1,3 butadiene, reaction sites of $C_{48}B_6N_6$ present electrophilic nature, surely. In each of the reaction channels, interaction between the most electrophilic and nucleophilic centers is favored. That is, in the B—C and B—N channels the most electrophilic site $\mathbf{B}_2$ prefers to interact with the most nucleophilic site $\mathbf{C}_5$ and produces regioisomer **16** and **25**, respectively. While in the N—C channel the most electrophilic site $\mathbf{C}_4$ chooses the most nucleophilic site $\mathbf{C}_5$ and produces regioisomer **36**. Predicted regioselectivity using local reactivity difference is in the agreement with the kinetic and thermodynamic results. Here new parameter can be defined, ΔR_k, as sum of the square of the differences between absolute values R_k at electrophilic centers and nucleophilic centers. ΔR_k for each of regioisomeric channels are as follows:

$$\Delta R_k^{15} = (0.421 - 0.055)^2 + (0.334 - 0.083)^2 = 0.197\,\text{eV}$$

$$\Delta R_k^{16} = (0.421 - 0.083)^2 + (0.334 - 0.055)^2 = 0.192\,\text{eV}$$

$$\Delta R_k^{25} = (0.421 - 0.083)^2 + (0.334 - 0.028)^2 = 0.207\,\text{eV}$$

$$\Delta R_k^{26} = (0.334 - 0.083)^2 + (0.421 - 0.028)^2 = 0.217\,\text{eV}$$

$$\Delta R_k^{35} = (0.421 - 0.028)^2 + (0.334 - 0.052)^2 = 0.234\,\text{eV}$$

$$\Delta R_k^{36} = (0.334 - 0.028)^2 + (0.421 - 0.052)^2 = 0.229\,\text{eV}$$

When the ΔR_k values are plotted toward corresponding activation Gibbs free energies, an acceptable correlation ($R^2 = 0.8809$) can be observed (see Fig. 6). As can be seen in Fig. 6, positive slope of the observed line suggests that the regioisomeric channel with the lower ΔR_k is faster and vice versa.

In order to illustrate the ability of the local electrophilicity and nucleophilicity in the determination of major regioisomer, structures of diene and dienophile together with the local nucleophilicity and electrophilicity values at the reaction sites are

Table 2
Electrophilic and nucleophilic YM Fukui functions, local electrophilicity, local nucleophilicity, local reactivity index and local softness for reaction sites of reactants.

k	f_k^+	f_k^-	ω_k	N_k	R_k	s_k^+	s_k^-
C_1	0.013	0.018	0.048	0.063	±0.055	0.005	
B_2	0.028	0.018	0.104	0.063	±0.083	0.011	
N_3	0.007	0.009	0.026	0.031	±0.028	0.002	
C_4	0.018	0.011	0.067	0.038	±0.052	0.007	
C_5	0.165	0.196	0.155	0.576	−0.421		0.034
C_6	0.179	0.171	0.168	0.502	−0.334		0.029

R_k values for carbon atom connected to the C_5 and C_6 are −0.231 and −0.160 eV, respectively.

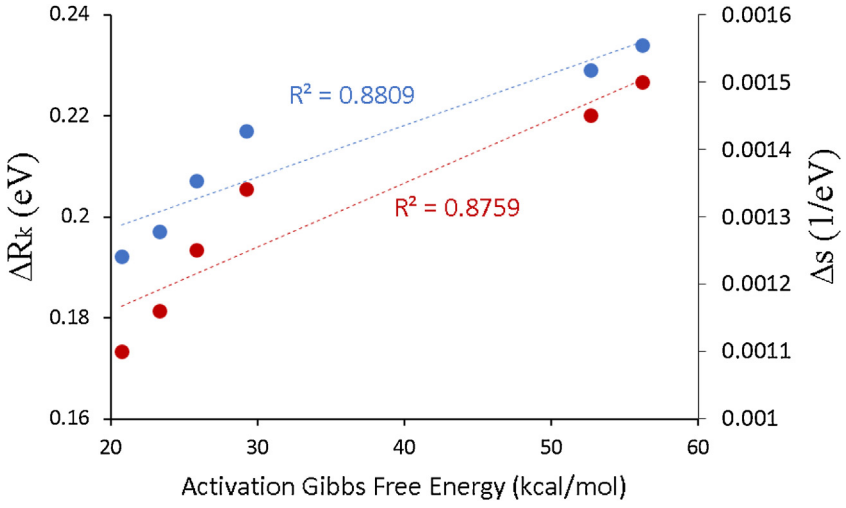

Fig. 6. Trend of ΔR_k (blue) and Δs (red) values with activation Gibbs free energy corresponding to the six regioisomeric channels. (For interpretation of the references to color in figure legend, the reader is referred to the web version of the article.)

depicted in Fig. 7. During a two-center interaction, the most favorable channel is related to the interaction between the most highly electrophilic center of the electrophile and the most highly nucleophilic center of the nucleophile [46]. In the 2-methyl-1,3 butadiene as diene the most nucleophilic center $\mathbf{C}_5$, $N_k = 0.576$ eV, reacts with the most electrophilic centers $\mathbf{B}_2$, $\omega_k = 0.104$ eV, and $\mathbf{C}_4$, $\omega_k = 0.067$. In fact, in the B—C pathway interaction between $\mathbf{C}_5$ of diene and $\mathbf{B}_2$ of dienophile (regioisomeric channel **16**), in the B—N pathway interaction between $\mathbf{C}_5$ of diene and $\mathbf{B}_2$ of dienophile (regioisomeric channel **25**) and in the N—C pathway interaction between $\mathbf{C}_5$ of diene and $\mathbf{C}_4$ of dienophile (regioisomeric channel **36**) are favored. The regioselectivity in the studied reactions can be explained using HSAB principle that recognized as Gazquez–Mendez [44] rule which stipulates that "the interaction between two chemical species is favored when it occurs through those atoms whose softnesses are approximately equal". Therefore, Δs values are calculated for both channels in each of heterobond pathways as follows:

$$\Delta s_{15} = (s^-_{C_5} - s^+_{C_1})^2 + (s^-_{C_6} - s^+_{B_2})^2 = 1.16 \times 10^{-3}\ \text{eV}^{-1}$$

$$\Delta s_{16} = (s^-_{C_5} - s^+_{B_2})^2 + (s^-_{C_6} - s^+_{C_1})^2 = 1.10 \times 10^{-3}\ \text{eV}^{-1}$$

$$\Delta s_{25} = (s^-_{C_5} - s^+_{B_2})^2 + (s^-_{C_6} - s^+_{N_3})^2 = 1.25 \times 10^{-3}\ \text{eV}^{-1}$$

$$\Delta s_{26} = (s^-_{C_5} - s^+_{N_3})^2 + (s^-_{C_6} - s^+_{B_2})^2 = 1.34 \times 10^{-3}\ \text{eV}^{-1}$$

$$\Delta s_{35} = (s^-_{C_5} - s^+_{N_3})^2 + (s^-_{C_6} - s^+_{C_4})^2 = 1.50 \times 10^{-3}\ \text{eV}^{-1}$$

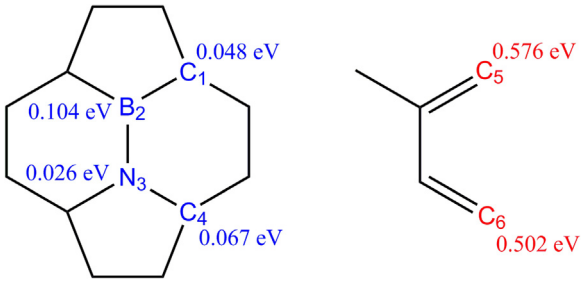

Fig. 7. Local nucleophilicity and electrophilicity values at the reaction sites of 2-methyl-1,3 butadiene and $C_{48}B_6N_6$ heterofullerene, respectively.

$$\Delta s_{36} = (s^-_{C_5} - s^+_{C_4})^2 + (s^-_{C_6} - s^+_{N3})^2 = 1.45 \times 10^{-3}\ \text{eV}^{-1}$$

So that $s^\alpha_k = Sf^\alpha_k$ and $\alpha = +, -$ refer to nucleophilic, electrophilic attack, respectively. S is the chemical softness and can be expressed as $S = 1/\eta$. It is clear that in each heterobond pathways the regioisomeric channel with lower activation Gibbs free energy corresponding to the major regioisomer is associated with smaller Δs value. Plotting of the Δs values toward the corresponding activation Gibbs free energies makes a straight line with an acceptable correlation ($R^2 = 0.8759$) (see Fig. 6), consequently regioisomeric channel with the lower Δs is faster and vice versa. High correlation between activation Gibbs free energies, ΔR_k and Δs values indicates that must be an acceptable correlation between ΔR_k and Δs values. When Δs is plotted toward ΔR_k an excellent correlation ($R^2 = 0.9992$) observed (see Fig. 8). This result shows that introduced parameter ΔR_k, can use to assign major and minor regioisomers and its ability is similar to Δs (Gazquez–Mendez rule).

Finally, prediction of major regioisomer in each of the heterobond pathways can be done by the FMO theory, in which bond formation takes place via an overlap between the relevant HOMO of nucleophile and the relevant LUMO of electrophile, so that the large–large and small–small FMO interactions are more favored than the large–small and small–large FMO interactions [48]. Calculated coefficients of relevant FMOs (see Fig. 9) at the B3LYP/STO-3G level show that the overlap process between relevant HOMO of 2-methyl-1,3 butadiene as diene and the relevant LUMO of dienophile leads to the formation of regioisomers **16** in the B—C heterobond

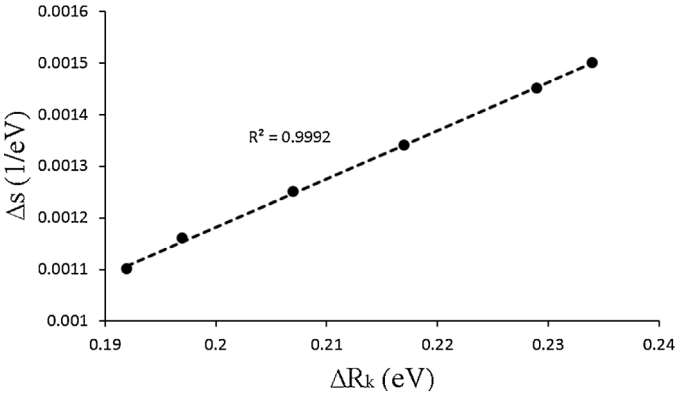

Fig. 8. Plot of the Δs versus the ΔR_k corresponding to the six regioisomeric channels.

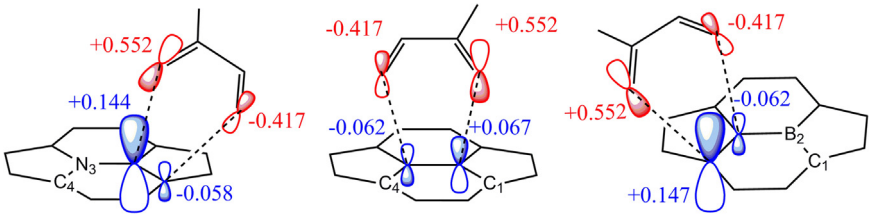

Fig. 9. Coefficients of relevant FMOs and the most favorable HOMO–LUMO interaction proposed by FMO theory.

pathway, **25** in the B—N heterobond pathway and **36** in the N—C heterobond pathway. This consequence is in complete agreement with activation parameters and DFT reactivity indices.

4. Final remarks and conclusions

The reaction mechanism and the regioselectivity of [4+2] Diels–Alder cycloaddition (**42C**) reaction of 2-methyl-1,3 butadiene with heterobonds of $C_{48}B_6N_6$ heterofullerene have been studied using DFT methods at the B3LYP/6-31G* level of theory. Because of electron deficient nature of the fullerene cages, such as C_{60}, in this work 2-methyl-1,3 butadiene and heterobonds of $C_{48}B_6N_6$ ($C_{48}B_6N_6$ is isoelectronic with C_{60}) are considered as diene and dienophile, respectively. Therefore, two regioisomers in each heterobond pathways can be produced. Kinetic and thermodynamic results show that B—C heterobond pathway is more active than B—N, and B—N heterobond pathway is more active than N—C. On the other hand in each explained heterobond pathways, regioisomers **16**, **25**, and **36** are major regioisomers. Generation of all regioisomers occur via one-step mechanism through asynchronous processes. Synchronicity values based on difference between two formed new single bonds between diene and dienophiles showed that TSs of B—N and B—C heterobond pathways have the greatest and the least synchronicity nature, respectively. The direction of the electron flux from 2-methyl-1,3 butadiene to $C_{48}B_6N_6$ heterofullerene along six studied pathways have been predicted by charge transfer calculations in the associated TSs and confirm the normal electron demand (NED) nature of investigated reactions. So, NED nature of the studied reactions is confirmed by global and local reactivity indices, electronic chemical potential, global electrophilicity, HOMO–LUMO energy gap between reactants, and local reactivity difference (R_k). R_k values show that the reaction sites of $C_{48}B_6N_6$ have ambiphilic character but in the presence of 2-methyl-1,3 butadiene, with nucleophilic activation active sites, $C_{48}B_6N_6$ reaction sites divulge only electrophilic nature, compulsorily. Predicted regioselectivities using R_k indice, Gazquez-Mendez rule and FMO theory are in complete agreement with the kinetic and thermodynamic results. Plotting of ΔR_k and Δs values of six studied channels toward corresponding activation Gibbs free energies showed that regioisomeric channel with lower ΔR_k and Δs is faster and vice versa. Interestingly, electronic and energetic results indicated that heterobond pathway B—C is more reactive than B—N and N—C as a result of higher bond order of B—C.

Appendix A. Supplementary data

Supplementary data associated with this article can be found, in the online version, at http://dx.doi.org/10.1016/j.jmgm.2014.08.003.

References

[1] W. Krätschmer, L.D. Lamb, K. Fostiropoulos, D.R. Huffman, Solid C60: a new form of carbon, Nature 347 (1990) 354–358.
[2] E. Zahedi, Adsorption of nitrogen dioxide on C30B15N15 heterofullerene: AIM and NBO study via DFT, C. R. Chim. 16 (2013) 189–194.
[3] M. Anafcheh, R. Ghafouri, F. Naderi, Exploring electronic structures for the most stable isomers of C12B6N6 and B6N6C12 heterofullerenes based on NMR, NICS and NBO analysis: a DFT study, Physica E 44 (2012) 1992–1998.
[4] M.R. Manaa, R.-H. Xie, J.V.H. Smith, Structure, vibrational and electronic spectra of heterofullerene C48(BN)6, Chem. Phys. Lett. 387 (2004) 101–105.
[5] K. Prassides, Physics and Chemistry of the Fullerenes, Kluwer Academic Publishers, NATO, 1994.
[6] A. Hirsch, M. Brettreich, Fullerenes, Chemistry and Reactions, Wiley-VCH Verlag, Weinheim, 2005.
[7] Y. Liang, Z. Shang, X. Xu, X. Zhao, Regioselectivity of 1,3-butadiene Diels–Alder cycloaddition to C59XH (X = N, B), Acta Phys. Chim. Sin. 24 (2008) 1811–1816.
[8] Z. Xiao, Y. Matsuo, M. Maruyama, E. Nakamura, Regioselective, [2+2] Cycloaddition of a fullerene Dimer with an alkyne triggered by thermolysis of an interfullerene C—C bond, Org. Lett. 15 (2013) 2176–2178.
[9] J.B. Briggs, G.P. Miller, [60] Fullerene–acene chemistry: a review, C. R. Chim. 9 (2006) 916–927.
[10] J. Yao, Z. Xiao, J. Zhang, X. Yang, L. Gan, W.-X. Zhang, Switched role of fullerene in the Diels–Alder reaction: facile addition of dienophiles to the conjugated fullerene diene moiety, Chem. Commun. (2009) 401–403.
[11] S. Osuna, J. Morera, M. Cases, K. Morokuma, M. Sola, Diels–Alder reaction between cyclopentadiene and C60: an analysis of the performance of the ONIOM method for the study of chemical reactivity in fullerenes and nanotubes, J. Phys. Chem. A 113 (2009) 9721–9726.
[12] B. Gonzalez, A. Herrera, B. Illescas, N. Martın, R. Martınez, F. Moreno, L. Sanchez, A. Sanchez, Diels–Alder cycloadducts of [60] fullerene with pyrimidine o-quinodimethanes, J. Org. Chem. 63 (1998) 6807–6813.
[13] P. Belik, A. Gügel, J. Spickermann, K. Müllen, Reaction of buckminsterfullerene with ortho-quinodimethane: a new access to stable C60 derivatives, Angew. Chem. Int. Ed. Engl. 32 (1993) 78–80.
[14] Y. Rubin, S. Khan, D.I. Freedberg, C. Yeretzian, Synthesis and X-ray structure of a Diels–Alder adduct of fullerene C60, J. Am. Chem. Soc. 115 (1993) 344–345.
[15] H.-T. Yang, X.-J. Ruan, C.-B. Miao, H.-T. Xi, Y. Jiang, Q. Meng, X.-Q. Sun, Hetero-Diels–Alder reaction of [60] fullerene with nitrosoalkene, Tetrahedron Lett. 50 (2009) 7337–7339.
[16] H.-T. Yang, W.-L. Ren, X.-J. Ruan, Z.-Y. Tian, X.-C. Liang, C. Han, X.-Q. Sun, C.-B. Miao, Reaction of [60] fullerene with α alkoxyl/acyloxyl/phenolyl ketoxime: unusual C—C and C—O bond cleavage, Tetrahedron Lett. 54 (2013) 1428–1431.
[17] N. Takahashi, T. Tajima, N. Tsugawa, Y. Takaguchi, Optically pure fullerodendron formed by diastereoselective DielseAlder reaction, Tetrahedron 66 (2010) 7787–7793.
[18] H. Kawakami, H. Okada, Y. Matsuo, Efficient, Diels–Alder addition of cyclopentadiene to Lithium ion encapsulated [60] fullerene, Org. Lett. 15 (2013) 4466–4469.
[19] S. Sato, Y. Maeda, J.-D. Guo, M. Yamada, N. Mizorogi, S. Nagase, T. Akasaka, Mechanistic study of the Diels–Alder reaction of paramagnetic endohedral metallofullerene: reaction of La@C82 with 1,2,3,4,5-pentamethylcyclopentadiene, J. Am. Chem. Soc. 135 (2013) 5582–5587.
[20] S. Osuna, M. Swart, J.M. Campanera, J.M. Poblet, M. Solà, Chemical reactivity of D3h C78 (Metallo)fullerene: regioselectivity changes induced by Sc3N encapsulation, J. Am. Chem. Soc. 130 (2008) 6206–6214.
[21] M. Cases, M. Duran, J. Mestres, N. Martin, M. Sola, The reactivity of the [5,6]-bond in cycloadditions to fullerenes, in: P.V. Kamat, D.M. Guldi, K.M. Kadish (Eds.), Fullerenes for the New Millennium, The Electrochemical Society. Inc., Pennington, NJ, 2001, pp. 244–269.
[22] A. Gugel, A. Kraus, J. Spickermann, P. Belik, K. Mullen, Buckminsterfullerene adducts from ortho-quinodimethanes, Angew. Chem. Int. Ed. Engl. 33 (1994) 559–561.
[23] S. Osuna, Theoretical Studies of the Exohedral Reactivity of Fullerene Compounds (Ph.D thesis), Universitate de Girona, 2009.
[24] L.S.K. Pang, M.A. Wilson, Reactions of fullerenes C60 and C70 with cyclopentadiene, J. Phys. Chem. 97 (1993) 6761–6763.
[25] M. Prato, V. Lucchini, M. Maggini, E. Stimpfl, G. Scorrano, M. Eiermann, T. Suzuki, F. Wudl, Energetic preference in 5,6 and 6,6 ring junction adducts of C60: fulleroids and methanofullerenes, J. Am. Chem. Soc. 115 (1993) 8479–8480.
[26] V.M. Rotello, J.B. Howard, T. Yadav, M.M. Conn, E. Viani, L.M. Giovane, A.L. Lafleur, Isolation of fullerene products from flames: structure and synthesis of the C60-cyclopentadiene adduct, Tetrahedron Lett. 34 (1994) 1561–1562.
[27] E. Emanuele, F. Negri, G. Orlandi, Structure, stability and spectroscopic properties of isomers of C48B6N6 heterofullerene with isolated and sequential BN substitutional patterns, Inorg. Chim. Acta 360 (2007) 1052–1062.
[28] A.D. Becke, Density functional thermochemistry. III. The role of exact exchange, J. Chem. Phys. 98 (1993) 5648–5652.

[29] R.G. Parr, W. Yang, Density Functional Theory of Atoms and Molecules, Oxford University Press, New York, 1994.
[30] W.J. Hehre, L. Radom, P.v.R. Schleyer, J.A. Pople, Ab initio Molecular Orbital Theory, Wiley, New York, 1986.
[31] H.B. Schlegel, Optimization of equilibrium geometries and transition structures, J. Comp. Chem. 3 (1982) 214–218.
[32] R. Seeger, J.A. Pople, Self-consistent molecular orbital methods. 28. Constraints and stability in Hartree–Fock theory, J. Chem. Phys. 66 (1977) 3045–3050.
[33] M.J. Frisch, G.W. Trucks, H.B. Schlegel, G.E. Scuseria, M.A. Robb, J.R. Cheeseman, G. Scalmani, V. Barone, B. Mennucci, G.A. Petersson, H. Nakatsuji, M. Caricato, X. Li, H.P. Hratchian, A.F. Izmaylov, J. Bloino, G. Zheng, J.L. Sonnenberg, M. Hada, M. Ehara, K. Toyota, R. Fukuda, J. Hasegawa, M. Ishida, T. Nakajima, Y. Honda, O. Kitao, H. Nakai, T. Vreven, J.A. Montgomery Jr., J.E. Peralta, F. Ogliaro, M. Bearpar, J.J. Heyd, E. Brothers, K.N. Kudin, V.N. Staroverov, R. Kobayashi, J. Normand, K. Raghavachari, A. Rendell, J.C. Burant, S.S. Iyengar, J. Tomasi, M. Cossi, N. Rega, J.M. Millam, M. Klene, J.E. Knox, J.B. Cross, V. Bakken, C. Adamo, J. Jaramillo, R. Gomperts, R.E. Stratmann, O. Yazyev, A.J. Austin, R. Cammi, C. Pomelli, J.W. Ochterski, R.L. Martin, K. Morokuma, V.G. Zakrzewski, G.A. Voth, P. Salvador, J.J. Dannenberg, S. Dapprich, A.D. Daniels, O. Farkas, J.B. Foresman, J.V. Ortiz, J. Cioslowski, D.J. Fox, Gaussian 09, Revision A.02-SMP, Gaussian, Inc., Wallingford, CT, 2009.
[34] R.G. Parr, L. von-Szentpaly, S. Liu, Electrophilicity index, J. Am. Chem. Soc. 121 (1999) 1922–1924.
[35] P.K. Chattaraj, S. Duleya, L.R. Domingo, Understanding local electrophilicity/nucleophilicity activation through a single reactivity difference index, Org. Biomol. Chem. 10 (2012) 2855–2861.
[36] T.A. Koopmans, Über die zuordnung von wellenfunktionen und eigenwerten zu den einzelnen elektronen eines atoms, Physica 1 (1934) 104–113.
[37] L.R. Domingo, M.J. Aurell, P. Perez, R. Contreras, Quantitative characterization of the global electrophilicity of common diene/dienophile pairs in Diels–Alder reactions, Tetrahedron 58 (2002) 4417–4423.
[38] L.R. Domingo, E. Chamorro, P. Pérez, Understanding the reactivity of captodative ethylenes in polar cycloaddition reactions. A theoretical study, J. Org. Chem. 73 (2008) 4615–4624.
[39] L.R. Domingo, P. Pérez, The nucleophilicity *N* index in organic chemistry, Org. Biomol. Chem. 9 (2011) 7168–7175.
[40] P. Jaramillo, L.R. Domingo, E. Chamorro, P. Pérez, A further exploration of a nucleophilicity index based on the gas-phase ionization potentials, J. Mol. Struct.: Theochem. 865 (2008) 68–72.
[41] R.G. Parr, W. Yang, Density functional approach to the Frontier-electron theory of chemical reactivity, J. Am. Chem. Soc. 106 (1984) 4049–4050.
[42] W. Yang, W.J. Mortier, The use of global and local molecular parameters for the analysis of the gas-phase basicity of amines, J. Am. Chem. Soc. 108 (1986) 5708–5711.
[43] R.K. Roy, S. Pal, K. Hirao, On non-negativity of Fukui function indices, J. Chem. Phys. 110 (1999) 8236–8245.
[44] J.L. Gazquez, F. Mendez, The hard and soft acids and bases principle: an atoms in molecules viewpoint, J. Phys. Chem. 98 (1994) 4591–4593.
[45] L.M. Giovane, J.W. Barco, T. Yadav, A.L. Lafleur, J.A. Marr, J.B. Howard, V.M. Rotello, Kinetic stability of the Ca-cyclopentadiene Diels–Alder adduct, J. Phys. Chem. 97 (1993) 8560–8561.
[46] L.R. Domingo, J.A. Saez, Understanding the mechanism of polar Diels–Alder reactions, Org. Biomol. Chem. 7 (2009) 3576–3583.
[47] E.D. Glendening, A.E. Reed, J.E. Carpenter, F. Weinhold, NBO Version 3.1.
[48] K.N. Houk, Frontier molecular orbital theory of cycloaddition reactions, Acc. Chem. Res. 8 (1975) 361–369.